Insight into the deactivation and regeneration of HZSM-5 zeolite catalysts in the conversion of dimethyl ether to olefins

Tomás Cordero-Lanzac*, Ainara Ateka, Paula Pérez-Uriarte, Pedro Castaño, Andrés T. Aguayo, Javier Bilbao

Department of Chemical Engineering, University of the Basque Country (UPV/EHU), PO Box 644-48080, Bilbao, Spain

Corresponding author: *tomas.cordero@ehu.eus*

ABSTRACT

The impact of different process variables affecting the coking and rejuvenation of HZSM-5 zeolite catalyst has been studied during the conversion of dimethyl ether (DME) to olefins in a fixed bed reactor. Those variables involve the effect of (i) the matrix material with mesopores; (ii) temperature; (iii) space time; (iv) acidity of the catalyst; (v) steam, inert or air in the reaction-regeneration medium. Used catalysts have been characterized through N_2 adsorption-desorption and temperature-programmed oxidation and the presence of three coke fractions has been identified deposited within the zeolite micropores, the external surface of the crystals and the mesopores of the matrix. Low Si/Al ratios (140) and temperatures (350 ºC), and co-feeding water with DME, reduce the formation of coke within the zeolite micropores, favoring the stability of the catalyst. Reaction-regeneration cycles confirm that catalysts totally recover the activity through combustion of coke during a heating ramp up to 550 ºC.

Keywords: Deactivation; Coke characterization; Regeneration; Dimethyl ether; Olefins

1. Introduction

Conversion of dimethyl ether (DME) is an attractive alternative for the sustainable production of olefins in order to progressively replace the classic routes of oil derived cracking.[1,2] DME is commonly obtained through dehydration of methanol, which is synthesized from the syngas produced by natural gas, coal, biomass or waste gasification/reforming.[3] Its direct production in a single stage with a bifunctional catalyst (syngas to DME or STD process) has marked thermodynamic advantages since the conversion of methanol to DME displaces the equilibrium of methanol synthesis.[4,5] Apart from the higher valorization of syngas directly transformed into DME, the conversion of co-fed CO_2 is also higher in STD process than that observed in a sequenced two-step synthesis of methanol and methanol dehydration to DME.[5–7] For this reason, STD process is considered one of the most encouraging and prospective route for the valorization of biomass and CO_2 at large scale.[8–10] On the other hand, DME presents interest not only as raw material for the production of olefins, but also from an economic point of view due to its potential use as household and engine fuels,[11,12] and hydrogen vector.[13–15]

Recent works on the transformation of DME into light olefins are focused on establishing a suitable catalyst and conditions for DTO process (DME to olefins),[16–19] with the aim of developing a feasible alternative to the implemented MTO process.[20] Results highlight a similar kinetic scheme for DTO and MTO processes over catalysts based on HZSM-5 zeolite or SAPOs (-18 and -34). This kinetic scheme follows the dual cycle mechanism (based on the hydrocarbon pool, HCP), which is reasonably well-explained and accepted in the literature.[21–24] According to this mechanism, methanol is transformed into a pool of organic intermediates (active species that include poly-

methyl benzenes and poly-methyl cyiclopentenyl cations), which form light olefins (primary gaseous products) through arenes dealkylation cycle and olefins oligomerization-cracking cycle.[24–28] Light olefins also undergo secondary reactions of hydride transfer, cyclization and condensation, thus forming paraffins, long chain olefins, aromatics and finally coke.[23,28–31] However, notable differences are also observed in the transformation of DME with respect to that of methanol to olefins.

Higher advance of the reaction and deactivation rates are reported for the transformation of DME using HZSM-5 zeolite.[29,30] DME is more reactive than methanol due to its higher proton affinity[32] and its ability to easily react with methoxy species (formed by adsorption of methanol and DME in the acidic sites), yielding propylene.[33] Experiments with the same content of water in the reaction medium also proved the higher reactivity of DME using this zeolite.[18] Nevertheless, shape selectivity and reaction conditions have a strong influence on the reactivity of both oxygenates. Li et al.[34] observed a higher reactivity of methanol (yielding product and coke) using a SAPO-34 catalyst and very low partial pressure of the reactant. At similar reaction conditions and catalyst acidities, the higher reactivity of DME over the HZSM-5 zeolite is attributed to the easy evolution of the dual cycle mechanism towards hydrocarbons due to the lower steric constraints.[17]

The differences between the conversions of DME and methanol suggest that distinct catalysts and conditions are required for maximizing the production of olefins and the stability of the catalyst. In a previous work, the great kinetic performance (activity, selectivity and stability) of HZSM-5 zeolite with high Si/Al ratio was reported.[17,18] Likewise, a kinetic model of the DME transformation into olefins was previously established, allowing for predicting the evolution of products with time on stream.[29,30] In this work, the deposition of coke in a HZSM-5 zeolite-based catalyst during the DME

conversion is studied, as well as its regeneration through combustion of coke. The main goal is to understand the influence of the catalyst properties (agglomeration of the zeolite in a matrix and acidity) and the reaction conditions (temperature, space time and DME dilution with N_2 or water) on the amount, nature and location of deposited coke, its effect on catalyst deactivation and thereby establishing the conditions for its complete removal. In this regard, catalyst deactivation and regeneration are intrinsically related and play a key role in the development of DTO process using a circulating fluidized bed reactor-regenerator system (like the MTO process does).[20]

2. Experimental

2.1. Catalyst preparation

Catalysts were prepared through wet extrusion of commercial HZSM-5 zeolites (with Si/Al molar ratios of 15 and 140) supplied by Zeolyst International. Pseudoboehmite (Sasol Germany) was used as a binder (30 wt% in the final catalyst), whereas a colloidal dispersion of α-alumina (Alfa Aesar, 22 wt%) was used as inert filler (20 wt% in the final catalyst). After a homogeneous mix of the components was reached, the extrudates were prepared and then dried at room temperature for 12 h, and at 110 ºC in a vacuum-dryer for 2 h. This agglomerated catalyst was sieved to a particle size between 0.125 and 0.3 mm and calcined at 575 ºC for 2 h using a temperature ramp of 5 ºC min^{-1}. During the thermal treatment, pseudoboehmite is transformed into γ-Al_2O_3. The zeolites were named by indicating their Si/Al molar ratio (Z15 and Z140), whereas the nomenclature for final catalysts was built by adding a C (CZ15 and CZ140).

2.2. Experimental runs

Reaction runs were carried out in an automated reaction equipment (PID Technology, Madrid, Spain) based on a stainless-steel fixed bed reactor heated by a cylindrical ceramic oven. The catalyst was mixed with inert SiC (with a particle diameter between 0.5 and 0.6 mm) in order to ensure a constant catalytic bed height in all experiments and isothermal conditions. Before the reactions, the catalyst was submitted to a pretreatment at 550 ºC for 2 h under a continuous flow of air (30 cm^3STD min^{-1}) for the sake of sweeping water and impurities trapped within the pores of the catalyst. The following reaction conditions were used: 325-400 ºC; 1.5 bar; space time, up to 2.0 g_{cat} h mol_C^{-1}; time on stream, 15 h. DME was fed diluted in N_2 and water, using a maximum DME-to-diluents molar ratio of 1:8 (DME partial pressure, 0.16 bar).

For catalyst regeneration experiments, reaction-regeneration cycles were carried out. After each reaction run, the catalytic bed was submitted to a sweeping with N_2 at the reaction temperature (350 or 400 ºC) for 10 min. Subsequently, the temperature was raised up to 550 ºC at 5 ºC min^{-1} under a continuous flow of air (30 cm^3STD min^{-1}). This temperature has proven to be suitable for the regeneration of catalysts calcined at 575 ºC, and used for the conversion of methanol and ethanol to hydrocarbon, avoiding the irreversible deactivation by dealumination.[35,36]

The reactor was coupled in-line with a gas chromatograph (Agilent 300A MicroGC) provided with four columns in order to identify the following reaction products: (i) CH_4 and CO in a MS-5 column; (ii) CO_2, DME and methanol in a Porapak Q column; (iii) C_2-C_5 paraffins and olefins in an Alumina column, and; (iv) C_6-C_8 paraffins and olefins and BTX aromatics in a Stabilwax column. Olefins, which are the main products of reactions, were grouped in a lump containing ethylene, propylene and butenes (*iso*-butene, 1-butene, *trans*-2-butene and *cis*-2-butene). The rest of hydrocarbons (C_{2-5} paraffins and BTX aromatics) were grouped in lumps named HC. Then, the conversion

of DME (X) and the yield (Y) of olefins and HC were defined in terms of carbon unit as:

$$X = \frac{F_C - F_{DME}}{F_C} 100 \quad (1)$$

$$Y_l = \frac{F_l}{F_C} 100 \quad (2)$$

where F_C is the total carbon molar flow in the reactor and F_{DME} and F_l are the carbon molar flows of DME (and methanol) and of *l* lump at the outlet of the reactor. Methanol is not considered a product of the DTO reaction since it is in equilibrium with DME at the reaction temperatures. A similar index based on the carbon atoms of olefins and the reactant is defined by Wei et al.[37] in order to describe the C atom economy. In our case, the yield of olefins corresponds to this C atom economy.

2.3. Used catalyst characterization

For assuring reproducible results of coke characterization, the catalytic bed was cooled to 150 ºC after each run and submitted to a sweeping with N_2 for 20 min in order to remove the adsorbed volatile products. Subsequently, the catalytic bed was cooled to room temperature and the catalyst was separated from the inert SiC for its characterization. The porous texture of the used catalysts was characterized by N_2 adsorption-desorption at -196 ºC. From the isotherms, the specific surface area (S_{BET}) was calculated using the BET equation, and the *t*-method was used to calculate the micropore volume ($V_{micropore}$) and the external surface area (S_t). In this case, S_t is associated with the external surface of zeolite crystals and the mesopores of the γ-Al_2O_3 matrix.

The total acidity of the zeolite, matrix and catalysts was determined by the adsorption-desorption of *tert*-butylamine (t-BA), combining thermogravimetric and differential

scanning calorimetry analyses in a Setaram TG-DSC calorimeter coupled to a mass spectrometer (Thermostar, Balzers). Samples were firstly submitted to a He stripping at 550 ºC, after which temperature was cooled down to 100 ºC and t-BA was adsorbed. Physisorbed molecules were removed by a He stripping, and then temperature was raised up to 500 ºC under the same He flux at 5 ºC min^{-1}. The t-BA desorption was monitored using the mass spectrometer by recording the signal of butene (m/z = 56), which is the main product of t-BA cracking.[38]

The content, location and nature of coke were studied by means of temperature-programmed oxidation (TPO) in a thermobalance TGA Q5000 IR (TA Instruments). Before the combustion, samples of used catalyst were submitted to a temperature-programmed desorption (TPD) in order to sweep water and reaction intermediates adsorbed on the surface of the catalyst. During TPD, temperature was stabilized in 50 ºC and then raised up to the reaction temperature of each used catalyst at a heating rate of 10 ºC min^{-1} in a continuous N_2 flow of 50 cm^3STD min^{-1}. After 15 min at this temperature, samples were cooled again at 50 ºC. The TPO analysis was carried out under an air flow of 50 cm^3STD min^{-1}, using a heating rate of 5 ºC min^{-1} up to 550 ºC and maintaining this temperature for 2 h

The weight loss during the TPO experiments is usually simulated with different kinds of models, but the simplest power-law kinetic models are generally used.[39–41] Moreover, Querini et al.[42] firstly explain the possibility of obtaining accurate fitting of experimental TPO profiles by their deconvolution with a linear combination of power-law expressions. According to our previous results,[30] three different coke fractions can be defined for describing the carbonaceous species deposited during DTO reactions. Their combustion was modeled assuming a complete combustion of each fraction, no diffusion limitations and a uniform combustion model of the coke particles. In this

sense, a power-law kinetic equation of first order, respect both each i coke fraction concentration (C_{Ci}) and oxygen partial pressure (P_{O2}), is defined:

$$-\frac{dC_{C_i}}{dt} = k_i^* \exp\left[-\frac{E_i}{R}\left(\frac{1}{T}-\frac{1}{T^*}\right)\right] C_{C_i} P_{O_2} \quad (4)$$

The kinetic constant was expressed using the reparameterized form of the Arrhenius equation. Thereby, k_i^* and E_i are the apparent kinetic constant at the reference temperature (T^*, 500 ºC) and the activation energy for the combustion of each i coke fraction, respectively, and R is the universal gas constant. The initial condition required for solving the ordinary differential equation is:

$$C_{C_i}\left(t=0\right) = f_i C_C \quad (5)$$

where f_i is the mass fraction of each i coke fraction and C_C is the total amount of coke calculated as the difference between the total mass of the used (after the TPD) and the regenerated catalyst (after the TPO). The optimal parameters of k_i^* and E_i were computed using a MATLAB routine, which allows for minimizing the sum of squares errors between experimental and calculated values as follows:

$$SSE = \sum_{j=1}^{n}\left[\left(\left.\frac{dC_C}{dt}\right|_{exp} - \sum_{i=1}^{3}\left.\frac{dC_{c_i}}{dt}\right|_{calc}\right)^2\right]_j \quad (6)$$

where j is the number of experimental point and n the maximum value of time in which a complete combustion of coke is observed.

3. Results and discussion

Catalyst deactivation by coking is crucial issue for the viability of DTO process and it is determined by the properties of the catalyst and the reaction conditions. The effect of

the properties of the catalyst (agglomeration of the zeolite in a mesoporous matrix and acidity) on the deposition of coke and its location in the catalyst particle is studied in the sections 3.1 and 3.2. The influences of the reaction conditions (temperature and space time) and of diluting the DME with N_2 and water are discussed in sections 3.3 and 3.4, respectively. Finally, section 3.5 deals with the study of catalyst regeneration in order to establish the combustion conditions for the complete recovery of the activity.

3.1. Effect of agglomerating the zeolite

The use of catalysts at industrial scale requires particles with high mechanical resistance. In general, zeolites present low particle size and mechanical resistance and, for this reason, they are usually embedded in a tougher matrix.[43] This changes the porous texture of the catalyst particle. Particularly, pseudoboehmite-derived mesoporous matrix provides the catalyst with a hierarchical porous texture, which favors the diffusion of reactants and is able to attenuate the blockage of the zeolite micropores.[43,44] **Table 1** shows the main textural parameters (calculated from the N_2 adsorption-desorption isotherms) of the bare zeolite with a Si/Al molar ratio of 15 (Z15), the pseudoboehmite-derived matrix (after the calcination at the same temperature than the catalyst, 575 ºC) and the final catalyst (CZ15). As it is possible to observe, the Z15 zeolite presents the highest value of BET specific surface area (S_{BET} of 436 $m^2\ g^{-1}$) with a minimum contribution of the specific external surface (S_t of 45 $m^2\ g^{-1}$). This result is typical of solids with a developed microporous texture ($V_{micropore}$ of 0.18 $cm^3\ g^{-1}$). On the contrary, pseudoboehmite-derived matrix exhibits a higher value of S_t than that of S_{BET} (131 and 113 $m^2\ g^{-1}$, respectively), which is associated with mesoporous solids without thinner pores than 2 nm (characteristic of γ-Al_2O_3). After the agglomeration, the textural parameter of the CZ15 catalyst (288 and 136 $m^2\ g^{-1}$ of S_{BET} and S_t, respectively) indicates that the microporous crystals of the zeolite are dispersed

in the mesoporous matrix, without decreasing the accessibility of N_2 towards its channels ($V_{micropore}$ of 0.06 cm^3 g^{-1}).

Table 1. Textural and acid parameters of the zeolite, the pseudoboehmite-derived matrix and the final catalysts from N_2 adsorption-desorption isotherms and t-BA adsorption-desorption.

	S_{BET} (m^2 g^{-1})	S_t (m^2 g^{-1})	$V_{micropore}$ (cm^3 g^{-1})	Total acidity ($mmol_{t\text{-}BA}$ g^{-1})
Z15	436	45	0.18	0.80
Matrix	113	131	0.00	0.12
CZ15	288	136	0.06	0.42
CZ140	271	131	0.07	0.33

Figure 1 displays the evolution of the conversion of DME with time on stream for the zeolite (Z15) and the catalyst (CZ15). Apart from the differences between the porous textures of both, the total acidity is almost two times higher for the Z15 zeolite (**Table 1**). Nevertheless, this is not a significant parameter in results of **Figure 1**, since the space time is referred to the amount of zeolite, i.e. the double weigh of CZ15 catalyst in the catalytic bed. The conversion of DME with the bare pseudoboehmite-derived matrix is negligible, and therefore its evolution is not depicted. As observed in **Table 1**, the total acidity of the matrix is lower than that of the CZ15 catalyst (0.12 $mmol_{t\text{-}BA}$ g^{-1}). Moreover, its acidic sites are weaker than those of Z15 zeolite,[45] which makes them non-actives in DTO reactions (neither products nor coke are observed). The initial conversions of the Z15 zeolite and the CZ15 catalyst are similar (44 and 50%, respectively). However, the decrease in the conversion with time on

stream is significantly faster for the Z15 zeolite. Both Z15 zeolite and CZ15 catalyst reach values of conversions lower than 5% after 15 h.

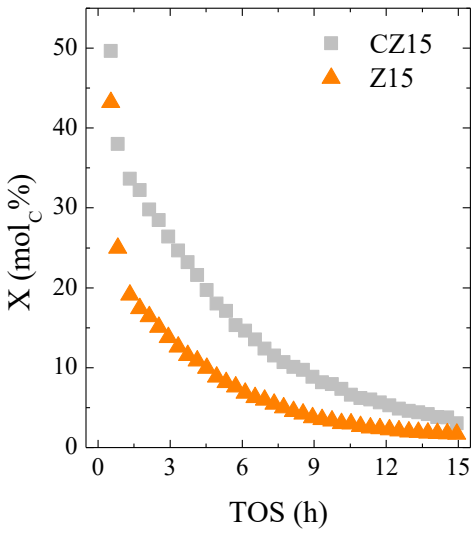

Figure 1. Comparison between the evolutions with time on stream of the conversion obtained with the zeolite (Z15) and the agglomerated catalyst in the pseudoboehmite-derived matrix. Reaction conditions: 350 ºC; space time 1.0 g_Z h^{-1} mol_C^{-1}.

In order to explain these results, TPO analyses were carried out with the CZ15 catalyst and Z15 zeolite used in runs with different temperatures and space time values. These TPO profiles were deconvoluted according to the combustion kinetic model previously described in the Section 2.3 and three different coke fractions (C1-C3) were defined. As an example, **Figure 2** shows the TPO profiles obtained for the CZ15 catalyst (**Figure 2a**) and the Z15 zeolite (**Figure 2b**) for a given reaction conditions. **Figure 2c** displays the corresponding values of total content of deposited coke (C_C) and the relative amount of each fraction (C1, C2 and C3).

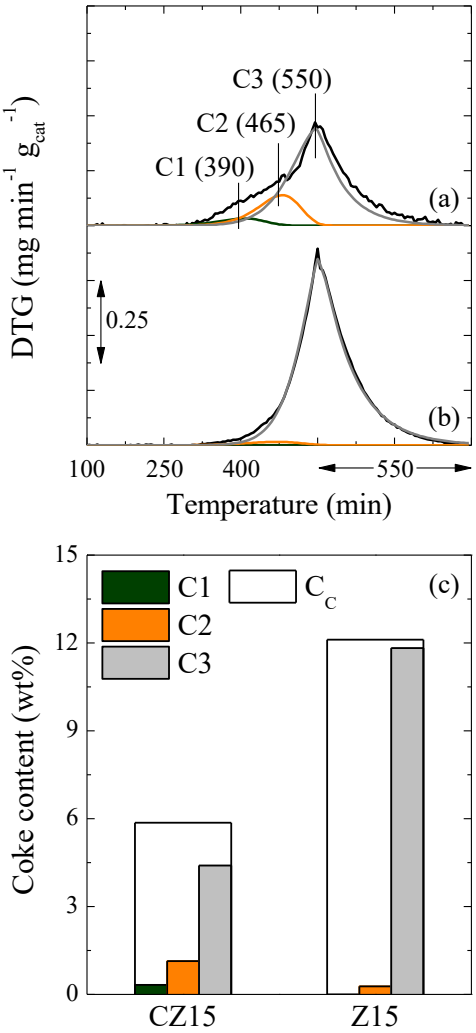

Figure 2. TPO profile deconvolutions for the used (a) CZ15 catalyst and (b) Z15 zeolite and (c) content of each coke fraction deposited on these catalysts

TPO profiles and coke fractions distribution of both used CZ15 catalyst and Z15 zeolite show clear differences, which are associated with the presence of the matrix in the catalyst. The one of the used CZ15 catalyst exhibits three peaks at ca. 390, 465 and 550 ºC (**Figure 2a**), attributed to the combustion of the coke fractions C1, C2 and C3, respectively. From the deconvolutions of the TPO profiles obtained for each zeolite-based catalyst (CZ15 and CZ140) using different temperatures and space time values, the apparent kinetic constant and activation energy of the combustion of each coke

fraction was computed (**Table 2**). Regarding the values of apparent kinetic constants of coke fractions C1, C2 and C3 (190, 61.1, and 7.56 atm^{-1} h^{-1}, respectively) and their activation energy (69.6, 88.9 and 144 kJ mol^{-1}, respectively), coke fractions easily burn following the order C1 > C2 > C3.

The existence of three coke fractions with different combustion rate deposited on the surface of an agglomerated HZSM-5 based catalyst has been related to their different location in the particle and composition.[45] Coke fractions C1 and C2 are located outside the microporous texture of the zeolite since they are not observed in the TPO of the bare zeolite (**Figure 2b**). Coke fraction C1, which exhibits low combustion temperature, is located on the mesoporous texture of the matrix and its formation is a consequence of the sweeping of the coke precursors from the acidic sites of the zeolite. Without the presence of the strong acidic sites of the zeolite, precursors of coke are deposited on the matrix surface but do not develop such a condensed structure. Consequently, it burns at this low temperature (390 ºC). Coke fraction C2 is associated with carbonaceous species located on the external surface of the zeolite crystals (presumably in the mouth of the zeolite channels). This can explain its intermediate values of combustion kinetic parameters (**Table 2**) and its minimum presence in the Z15 zeolite (**Figure 2c**), since the external surface of Z15 is very low (45 m^2 g^{-1}, **Table 1**).

In Z15 zeolite, the combustion of coke fractions C2 and C3 (orange and grey lines in **Figure 2b**) are overlapped inasmuch as zeolite crystals are not dispersed in a matrix but form clusters within which coke fraction C2 is also deposited. For this reason, coke fraction C3 is the only noticeable one in used Z15 zeolite. Its high combustion temperature (550 ºC) suggests that this coke fraction presents a developed and condensed structure. This is presumably a consequence of its formation over the acidic sites of the zeolite, thus partially blocking micropores (**Table 1**). Several authors

associated the formation of coke from methanol[28,46–48] and DME[45] with the condensation of polyalkyl aromatics (trapped in the channels of the zeolite) towards developed carbonaceous structures. Therefore, the location of this coke fraction C3 within the micropores of the zeolite (blocking the acidic sites) hinders its combustion, which could explain the position of the peak in the TPO profile and the values of the kinetic parameters.

Table 2. Kinetic parameters of the combustion of each coke fraction deposited in CZ15 and CZ140 catalysts.

	CZ15	**CZ140**
k_1 (atm^{-1} h^{-1})	$(1.90 \pm 0.25)\ 10^2$	$(1.68 \pm 0.20)\ 10^2$
k_2 (atm^{-1} h^{-1})	$(6.11 \pm 0.90)\ 10^1$	$(4.89 \pm 0.19)\ 10^1$
k_3 (atm^{-1} h^{-1})	$(7.56 \pm 1.23)\ 10^0$	$(1.01 \pm 0.09)\ 10^1$
E_1 (kJ mol^{-1})	$(6.96 \pm 1.25)\ 10^1$	$(8.10 \pm 0.31)\ 10^1$
E_2 (kJ mol^{-1})	$(8.89 \pm 2.50)\ 10^1$	$(1.07 \pm 0.07)\ 10^2$
E_3 (kJ mol^{-1})	$(1.44 \pm 0.21)\ 10^2$	$(1.16 \pm 0.04)\ 10^2$

According to the literature on the combustion of coke, the composition of each coke fraction could also be associated with their different combustion temperature. Several authors attributed higher combustion rate (coke fractions C1 and C2) with the presence of O-containing carbon structures[49,50]. Leistener et al.[51] also reported a linear correlation between the activation energy of each carbonaceous species and its C/H ratio. They found values of activation energy for coke in the same range that the ones we have

observed, and according to their results, the coke fraction C1 should have lower carbon content (more aliphatic) than those of coke fractions C2 and C3. In this regard, the latter presents the most condensed structures without oxygen due to the high activity of acidic sites for dehydrating and condensing components of coke.

Figure 2c also displays a double content of coke deposited in the CZ15 catalyst than that in Z15 zeolite. Hence, the content of coke per zeolite weight is similar in both cases (ca. 6 wt%). In consequence, the role of agglomerating the zeolite in a matrix is to modify the distribution of coke fractions, diminishing the content of coke fraction C3 and favoring the deposition of coke fractions C1 and C2 outside the zeolite in the mesopores of the matrix.

3.2. Effect of the Si/Al ratio de la zeolite

Figure 3a shows the evolution of the DTO conversion with time on stream for two agglomerated catalysts with different Si/Al molar ratio (CZ15 and CZ140) at 350 and 400 ºC. **Table 1** shows the total acidity values of both, being higher the one registered for the catalyst with lower Si/Al molar ratio (0.42 and 0.33 $mmol_{t\text{-}BA}\ g^{-1}$ for CZ15 and CZ140, respectively). In a previous work, the strong influence of Si/Al molar ratio on the amount of acidic sites in a HZSM-5 zeolite was demonstrated,[52] which is also reported by other authors.[53] It can be observed that the initial conversions are similar for both catalysts at the same temperature, thus yielding values of 28.4 and 25.6% at 350 ºC and of 99.5 and 89.5% at 400 ºC (for CZ15 and CZ140 catalysts, respectively). Nevertheless, the conversion decays much faster for the CZ15 catalyst (with higher acidity and acid strength), being remarkable the practically total loss of the activity after 4.5 h at 400 ºC (the remaining conversion of 2 % is the results of the thermal cracking of DME forming CO and CH_4). On the other hand, CZ140 catalyst presents a linear and

slower decay of the conversion, and losses ca. 10 % of the initial conversion at 15 h on stream at both temperatures.

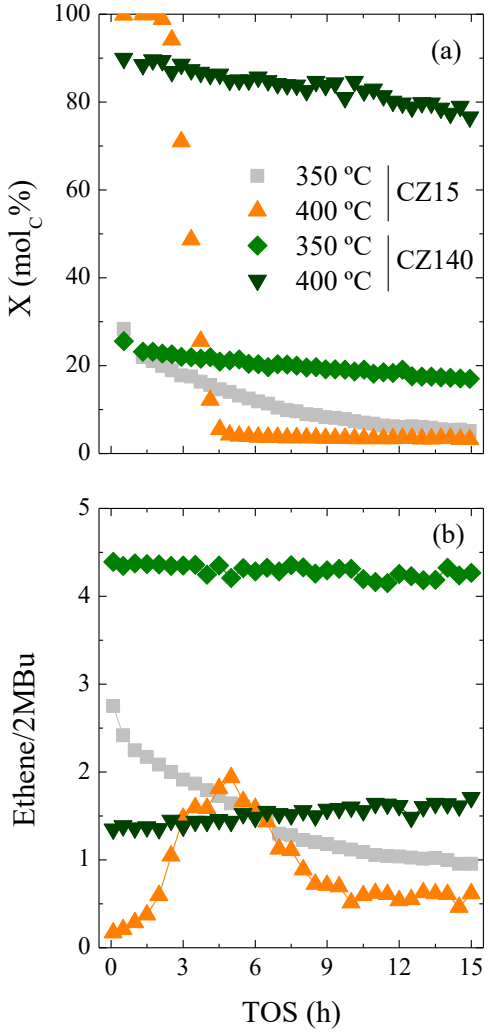

Figure 3. Evolution of (a) the conversion and (b) the Ethene/2MBu ratio with time on stream for the CZ15 and CZ140 catalysts at 350 and 400 ºC. Space time, 1.0 g_{cat} h^{-1} mol_C^{-1}.

An evaluation of the relative effect of deactivation on each of the cycles of olefin formation mechanism is carried out by following the Ethene/2MBu (2-methylbutane and 2-methyl-2-butene) ratio defined by Khare et al.[54] The evolution of this ratio with time on stream gives an estimation of the dominant cycle during the reaction. This way,

an increase in the Ethene/2MBu ratio represents an increase in the relative advance of the arene/alkene cycle ratio. Although this methodology only provides an overall approximation of the relative contribution of each cycle, it is a useful tool for understanding the product distribution in the conversion of methanol and DME into olefins. This ratio has been reported as particularly interesting for comparing experimental runs co-feeding reactants[23] or using catalysts with different Si/Al ratio.[54]

Figure 3b illustrates the evolution of Ethene/2MBu ratio with time on stream for the four runs depicted in **Figure 3a**. As we previously observed for this reaction,[45] a decrease in the reaction temperature leads to an increase in the Ethene/2MBu ration at zero time on stream and then to a promotion of the arene cycle. Regarding the zeolite acidity, the arene cycle is also favored when the catalyst presents lower acidity (CZ140 catalyst). At this point, low DTO conversions (achieved with low acid catalyst and/or at low temperature) could be associated with higher arene cycle contribution and olefins selectivity.

Regarding the evolution of Ethene/2MBu ratio with time on stream obtained with CZ140 catalyst (**Figure 3b**), constant and slightly increasing trends are observed at 350 ºC and 400 ºC, respectively. This suggests an increasing contribution of the arene cycle as the catalyst deactivation occurs. The higher Ethene/2MBu ratio registered for CZ140 catalyst than that for CZ15 one can also be associated with the higher stability of the first in this reaction. The decrease in the Ethene/2MBu ratio with the CZ15 catalyst upon increasing the time on stream at 350 ºC (**Figure 3b**) indicates an increase in the relative contribution of alkene cycle as the catalyst is deactivated. Interestingly, Ethene/2MBu ratio shows very low initial values and reaches a maximum using this catalyst at 400 ºC. This result can be attributed to the complete conversion observed during the first 3 h on stream, which means that the arene cycle (first stage of the

mechanism) has reached the thermodynamic regime. Consequently, the low value of Ethene/2MBu ratio is due to the advance of alkene cycle at these conditions. After this period, deactivation is noteworthy and the Ethene/2MBu ratio increases, pointing out a higher relative contribution of the arene cycle on the formation of products. Finally, deactivation also attenuates the advance of the arene cycle and the decreasing tendency of the Ethene/2MBu ratio is similar to that observed at 350 ºC with the same catalyst.

The different deactivation rate and product distribution of catalysts with different acidity could be explained by the formed coke fractions, which are observed in the TPO profile shapes of **Figure 4**. The TPO profiles of the used CZ140 catalyst (**Figure 4b** at 350 and 400 ºC) show a wider peak distributed in a higher range of temperature and with a maximum located at lower temperatures than the ones of used CZ15 catalyst (**Figures 4a** at 350 and 400 ºC). Therefore, a coke with a more heterogeneous nature is deposited on the surface of CZ140 catalyst. This also leads to a little discrepancy between the kinetic parameters of the combustion of each coke fraction deposited in both catalysts (**Table 2**). In this sense, the apparent kinetic constant of the combustion of the coke fractions C1 and C2 decreases and their activation energy increases when the acidity of the catalyst is lower (CZ140 catalyst). However, the combustion of the coke fraction C3 shows a higher apparent kinetic constant (10.1 atm^{-1} h^{-1}) and a lower activation energy (116 kJ mol^{-1}), which means that it is easily burnt off. This is in accordance with the lesser capability of condensing species of coke exhibited by the weaker acidic sites.

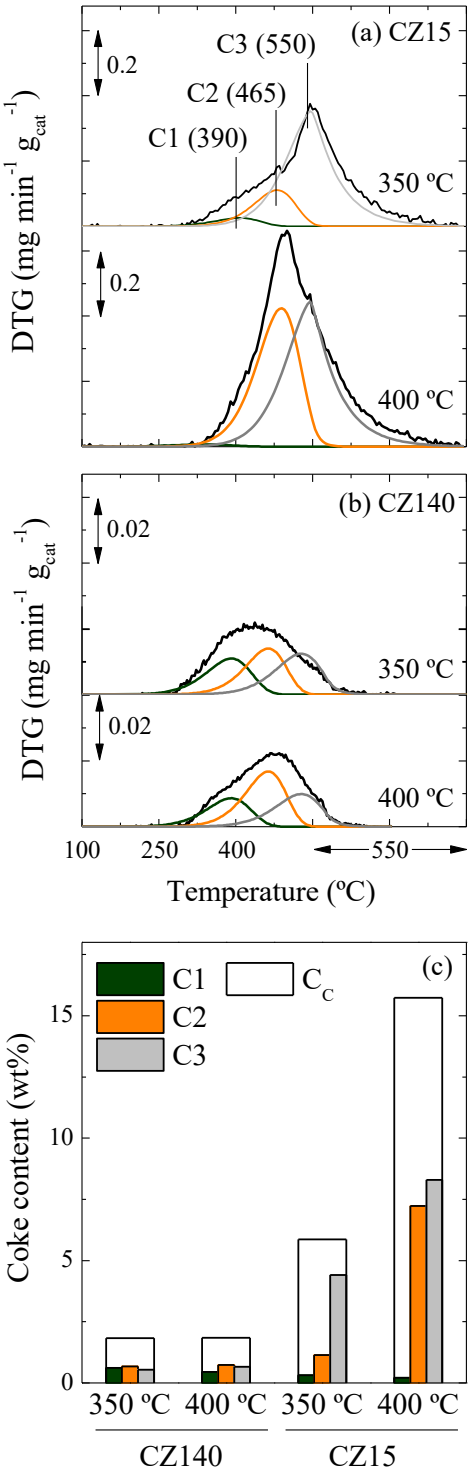

Figure 4. TPO profile deconvolutions for the used (a) CZ15 and (b) CZ140 catalysts at 350 ºC and 400 ºC, and (c) content of each coke fraction deposited on these catalysts.

The textural parameters of used catalysts, displayed in **Table 3**, corroborate the previously discussed location of this coke fraction C3 within the micropores of the zeolite (**Table 1**). The values S_t calculated for the CZ15 catalyst at both temperatures are similar, or even higher, than those of S_{BET}. That means that the used catalysts present a totally blocked microporous texture but shows certain external surface. On the contrary, the used CZ140 catalysts present higher specific surface area with a considerable contribution of micro- and mesopores ($S_{BET} > S_t$). The lower blockage of the zeolite micropores is in accordance with the lower activity loss, the lower content of coke and the more heterogeneous nature of coke (with lower amounts of coke fraction C3) exhibited by the CZ140 catalyst. The total acidity values of the used catalysts are also consistent with the discussed textural parameters (**Table 3**), showing the used CZ140 catalysts higher values at both temperatures.

Table 3. Textural and acid parameters of the used CZ15 and CZ140 catalyst at different reaction conditions from N_2 adsorption-desorption isotherms and t-BA adsorption-desorption.

	S_{BET} ($m^2\ g^{-1}$)	**S_t ($m^2\ g^{-1}$)**	**$V_{micropore}$ ($cm^3\ g^{-1}$)**	**Total acidity ($mmol_{t\text{-}BA}\ g^{-1}$)**
CZ15				
350 ºC; 0.5 $g_{cat}\ h^{-1}\ molC^{-1}$; Pure DME	94	108	0.00	0.10
350 ºC; 1.0 $g_{cat}\ h^{-1}\ molC^{-1}$; Pure DME	91	90	0.00	0.11
350 ºC; 1.0 $g_{cat}\ h^{-1}\ molC^{-1}$; 1:2 (DME:$N_2$)	89	105	0.00	0.09
350 ºC; 1.0 $g_{cat}\ h^{-1}\ molC^{-1}$; 1:2 (DME:$H_2O$)	127	119	0.01	0.15
400 ºC; 1.0 $g_{cat}\ h^{-1}\ molC^{-1}$; Pure DME	74	85	0.00	0.06
CZ140				
350 ºC; 1.0 $g_{cat}\ h^{-1}\ molC^{-1}$; Pure DME	180	117	0.03	0.20
400 ºC; 1.0 $g_{cat}\ h^{-1}\ molC^{-1}$; Pure DME	192	105	0.04	0.24

The total content of coke and the ones of each fraction (**Figure 4c**) can also be related to the evolution of the Ethene/2MBu ratio with time on stream depicted in **Figure 3b**. The increase in the temperature with CZ140 catalyst does not significantly change the amount of deposited coke (ca. 1.9 wt% at both temperatures in **Figure 4c**). However, a slight increase in the amount of coke fraction C3 can be observed, which could be attributed to the condensation of the hydrocarbon pool species. This situation corresponds to the higher relative contribution of the alkene cycle observed in **Figure 3b** at high temperature. On the other hand, the used CZ15 catalyst exhibits higher contents of coke and particularly of coke fraction C3 deposited within the micropores of the zeolite, which is presumably explained by the faster degradation of the species involved in the dual cycle mechanism. Although coke fraction C3 is responsible of the fast-initial deactivation, it is also significant the important increase in the coke fraction C2 at 400 ºC that points out the deposition of coke outside the zeolite crystals.

3.3. Effect of the reaction conditions

For discussing the effect of reaction conditions on the coke deposition and catalyst deactivation, runs were carried out using different temperatures and space time. **Figure 5** shows the evolution of the total content of coke and the one of each coke fraction deposited in the CZ15 (**Figure 5a**) and CZ140 (**Figure 5b**) catalysts from a reaction temperature of 325 to 400 ºC. Moreover, **Figure 6** illustrates the evolution of the conversion with time on stream for these runs. Regarding the results obtained with the CZ15 catalyst, the total coke content increases when the reaction temperature is raised, however an opposite trend is observed for the coke fraction C1, which significantly drops (**Figure 5a**). Likewise, an increment of the temperature leads to increases in the conversion and deactivation rate (**Figure 6a**). Thereby, the results of coke formation rate and advance of DTO reaction could be associated. Coke is

predominantly formed within the channels of the zeolite (coke fraction C3), which could diffuse outside them when the amount of deposits is relatively high (coke fraction C2, with remarkable concentration at 400 ºC). After 6 h, acidic sites are almost deactivated for the formation of olefins (**Figure 6a**), but they show a residual activity for the methylation of polyalkyl aromatics and the formation of coke. Lastly, the fast rate of condensation of this intermediates at high temperatures could explain the lower migration of deposits to the mesoporous matrix at this condition (coke fraction C1).

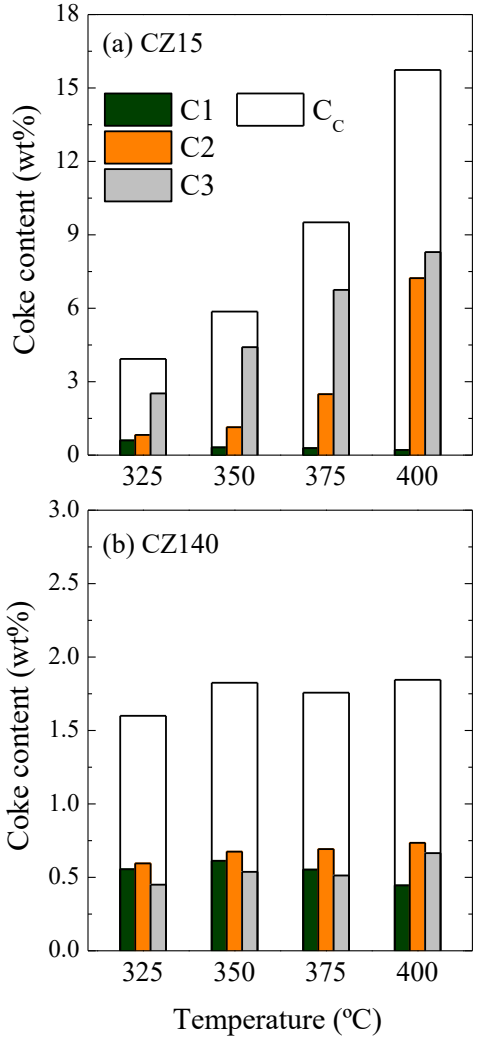

Figure 5. Evolution of the content of each coke fraction with temperature for the used (a) CZ15 and (b) CZ140 catalysts (Space time, 1.0 g_{cat} h^{-1} mol_C^{-1}).

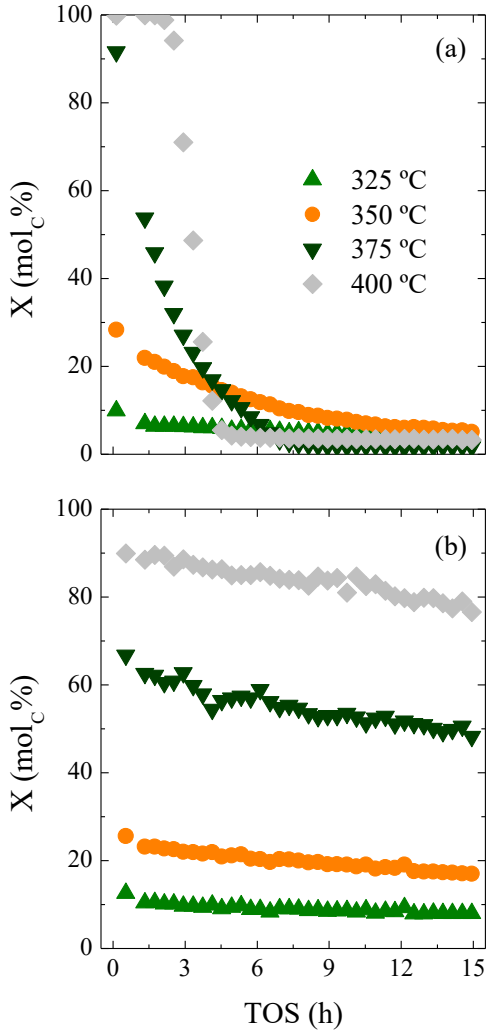

Figure 6. Effect of reaction temperature on the evolution of the conversion with time on stream for the (a) CZ15 and (b) CZ140 catalysts. Space time, 1.0 g_{cat} h^{-1} mol_C^{-1}.

The lower acidity of CZ140 catalyst has a strong influence on the deposition of coke (**Figure 5b**) and on the decay of the conversion with the time on stream (**Figure 6b**), which is slower than that observed with CZ15 catalyst (**Figure 6a**). Although the initial activity of the CZ140 catalyst is lower, the also lower density and strength of the acidic sites hinder the direct formation of coke through oligomerization of olefins.[45,55,56] **Figure 5b** shows different coke fraction distribution in both catalysts, being the coke fraction C3 the main one deposited on the CZ15 catalyst. On the contrary, the formation

of coke fractions C1 and C2 is favored by the lower activity of CZ140 catalyst for condensing olefins and retaining polyaromatics within its channels.

According to these results, mild conditions, such as moderate acidity or low temperature (350 ºC), allow for controlling the advance of the reaction and the formation of coke. In these cases, the main cause of deactivation should be the mask of acidic sites by coke (observe the decrease of total acidity in **Table 3**). The straight and relatively wide channels of MFI framework ease the sweeping of the precursors of coke, thus delaying the formation of polyaromatic structures that block the zeolite pores. This total blockage of micropores is reported as the main cause of deactivation of a SAPO-34 catalyst during the conversion of methanol,[57,58] and it is also observed in our reaction when conditions were harsher (high acidity and 400 ºC). A negligible value of $V_{micropore}$ and very low one of total acidity (0.06 $mmol_{t\text{-}BA}$ g^{-1}) is registered at these conditions (**Table 1**). It is worth of mentioning that the similar $V_{micropore}$ values could be associated with the conditions of porous texture characterization (-196 ºC) that can homogenize the coke of all used catalysts. Using DME as reactant, lower temperatures and acidity can be used due to its higher reactivity, which leads to a lower advance of condensation reactions.

Modifying the space time allows for studying the advance of the reaction, which gives information about the advance of the mechanisms of coke formation. **Figure 7a** depicts the effect of the space time on the coke content and the ones of each fraction using the CZ15 catalyst at 375 ºC. The evolution of product distribution at these conditions is depicted in **Figure 7b**. The total content of coke increases from 3.7 to 9.5 wt% for space time values of 0.25 and 1.0 g_{cat} h mol_C^{-1}, respectively, and coke fraction C3 is predominant in all cases (**Figure 7a**). Otherwise, this coke fraction represents an 80% of the coke deposited at low space time (low advance of the reaction). This result is

consistent with the previously proposed hypothesis of coke formation over the acidic sites within the zeolite crystals and the precursors sweeping to the inert matrix, thus yielding the coke fractions C1 and C2. The low value of total content of coke exhibited for a space time value of 0.25 g_{cat} h mol_C^{-1} (**Figure 7a**) is related with maxima concentrations of DME in the reaction medium (**Figure 7b**). This suggests that DME has a lower impact on the formation of coke compared with other products. By rising the space time, the content of all coke fractions increases in parallel with the following reaction medium evolution: a decay of DME concentration and an increase in the yields of olefins, paraffins and BTX aromatics. The maximum of coke content and olefins concentration observed for a space time value of 1.0 g_{cat} h mol_C^{-1} suggests that these species are the main precursors for the formation of coke.

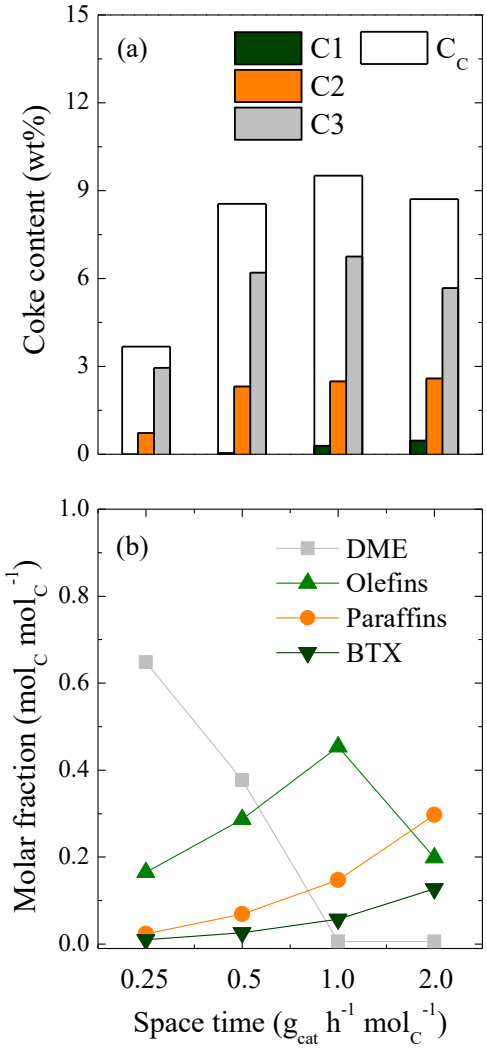

Figure 7. (a) Evolution with space time of (a) the content of each coke fraction and (b) the product distribution for the CZ15 catalysts at 375 ºC

3.4. Effect of DME dilution

The encouraging interest of co-fed water for mitigating the catalyst deactivation in the conversion of methanol is well-established in the literature,[59–61] and in fact, this strategy is used at industrial scale in MTO process.[20] This attenuation of deactivation has also been observed in the conversion of DME[18,30] and has been attributed to several factors: (i) the reduction of the partial pressure of reactants, which delays the advance of the reaction; (ii) the competitive adsorption of water and coke precursors on the acidic sites,

and; (iii) the sweeping of the precursors of coke from the zeolite to the mesoporous matrix. Additional DTO runs were carried out by diluting DME with water (maintaining the same space time referred to C units, 1.0 g_{cat} h^{-1} mol_C^{-1}) for determining its influence on the deposition of coke and on the catalyst deactivation. **Figure 8** shows the total content of coke and the one of each fraction using the CZ15 catalyst and co-feeding N_2 or H_2O with DME at 350 ºC (**Figure 8a**) and 400 ºC (**Figure 8b**).

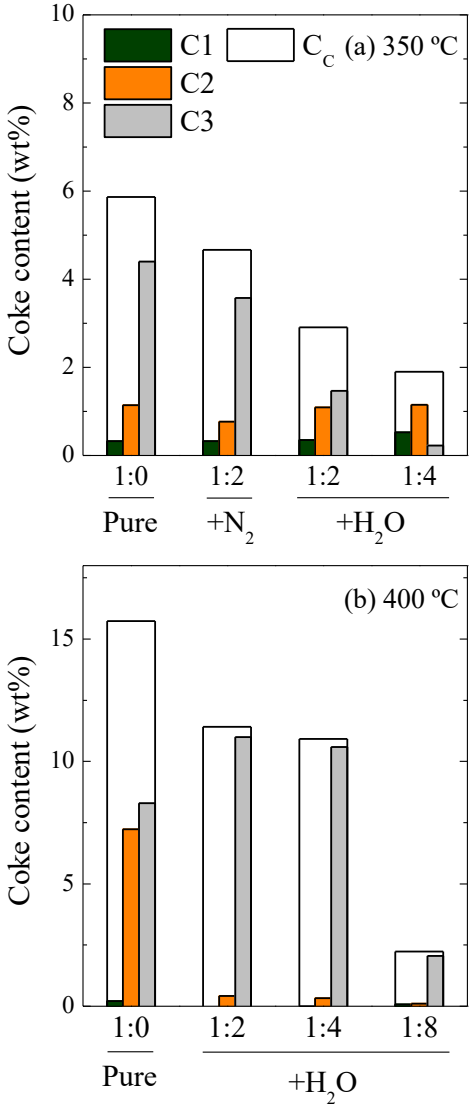

Figure 8. Evolution of the content of each coke fraction with the DME dilution with N_2 or H_2O using the CZ15 catalyst at (a) 350 ºC and (b) 400 ºC. Space time, 1.0 g_{cat} h^{-1} mol_C^{-1}.

Co-feeding N_2 with DME leads to a decrease in the total content of coke (**Figure 8a**) due to the lower advance of DTO reaction as a consequence of the reduction of DME concentration.[29] This also provokes a drop of the initial conversion but it is worth of mentioning the slightly decrease of deactivation rate achieved following this dilution strategy (**Figure 9a**). In contrast, the effect of co-feeding water at 350 ºC presents higher impact on the deposition of coke and the attenuation of catalyst deactivation. A pronounced drop of the coke fraction C3 (and consequently of the total content of coke) is observed using a DME/H_2O molar ratio of 1:2 (**Figure 8a**). The promoted sweeping by steam of the precursors of coke to the mesopores of the matrix and their competitive adsorption over the acidic sites could explain this interesting result, as well as the increase in the relative concentration of coke fractions C1 and C2. This intermediates swept, which unblocks the acidic sites, leads to the aforementioned decay of the initial conversion but allows reaching a steady conversion state using a DME/H_2O ratio of 1:4 (**Figure 9a**). Textural and acid parameters are in concordance with this hypothesis (**Table 3**). As observed, the values obtained for the catalyst used with a DME/N_2 molar ratio of 1:2 are similar to those registered for pure DME. However, co-feeding water with a DME/H_2O ratio of 1:2 yields a used catalyst with higher S_{BET} and some remaining accessible micropores ($S_{BET} > S_t$ and $V_{micropore} > 0$), which could explain the higher values of conversion after 15 h on stream.

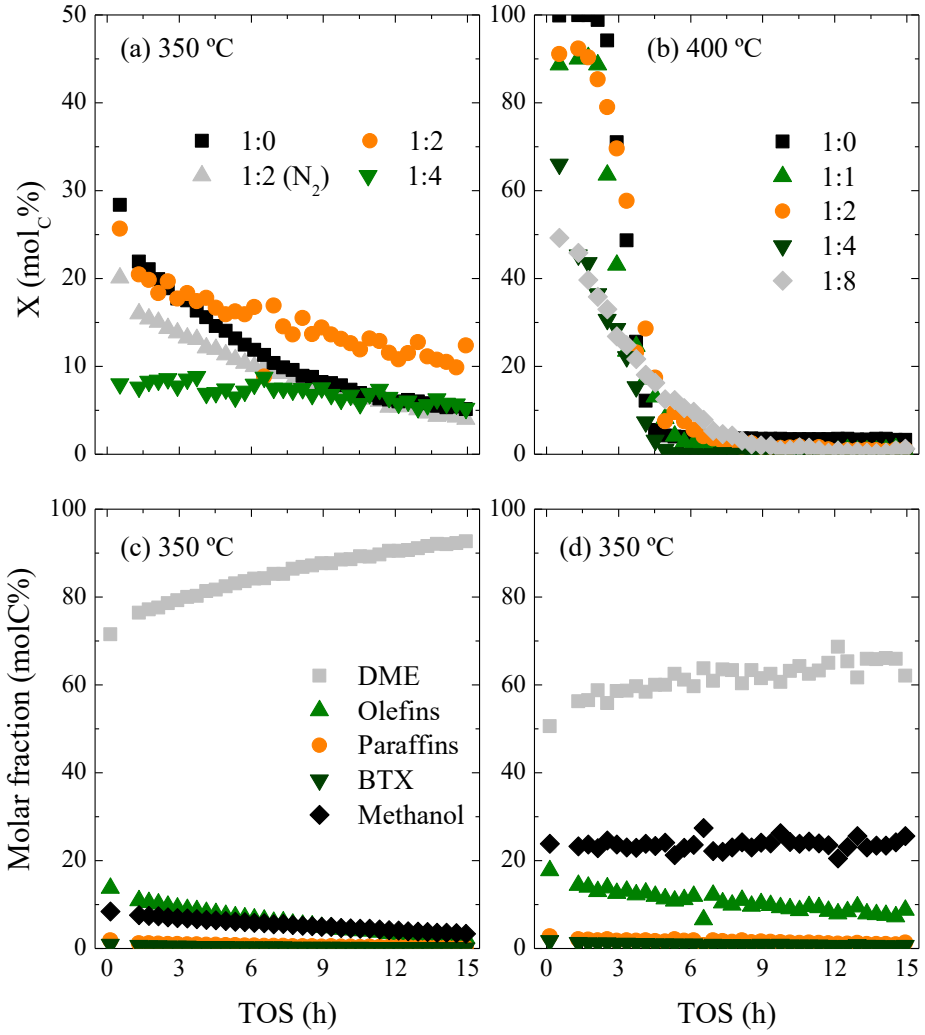

Figure 9. Effect of DME dilution with N_2 and H_2O on the evolution with time on stream of the conversion at (a) 350 and (b) 400 ºC and of the product distribution at 350 ºC for (c) DME:N_2 ratio of 1:2 and (d) DME:H_2O ratio of 1:2. CZ15 catalyst; space time, 1.0 g_{cat} h^{-1} mol_C^{-1}.

The previously discussed influence of co-feeding H_2O with DME on the catalyst deactivation is stronger than that observed in the conversion of methanol[59–61] since pure methanol tends to easily dehydrate to DME, forming water at the inlet of the reactor. Consequently, the strategy of co-feeding water turns out interesting in the conversion of

DME despite the conversion and product distribution can significantly change with the DME/H_2O ratio (**Figures 9c** and **9d**).

Increasing the temperature up to 400 ºC, a similar tendency is observed in the deposition of coke (**Figure 8b**). A reduction of the total content of coke from 15.7 to 2.2 wt% is achieved with a DME/H_2O molar ratio of 1:8. Nevertheless, the coke is mainly located within the micropores of the zeolite (coke fraction C3), leading to a relatively fast catalyst deactivation, and a situation of catalytic stability is not reached at this higher temperature (**Figure 9b**). Steam seems to favor the sweeping of coke precursors (coke fraction C1 and C2 are not observed for high DME:H_2O molar ratios, **Figure 8b**) but does not avoid the oligomerization and condensation mechanisms that lead to catalyst deactivation. Therefore, reaction temperature also plays a key role in the influence of water on the deposition of coke. At 400 ºC, the high activity of this catalyst, which rapidly forms the reaction intermediates and coke precursors, makes more difficult to attenuate the coke deposition inside the zeolite crystals. Undoubtedly, the high acidity of CZ15 catalyst presumably contributes to this outstanding activity of condensing coke at 400 ºC (**Figure 4c**).

3.5. Catalyst regeneration

Regenerability is one of the most important properties of the catalyst from an operating feasibility point of view. Particularly, it is crucial in acid-catalyzed reaction, such as catalytic cracking (FCC) or MTO, in which deactivation by coking is fast. Although a complete combustion of deposited coke is observed at 550 ºC (**Figures 2** and **4**), this does not necessary mean a total recovery of the catalytic activity. In this regards, cycles of reaction-regeneration were carried out with both catalysts and different conditions of reaction and regeneration. **Figure 10** shows the evolution with time on stream of the DTO conversion and the yields of olefins and the rest of hydrocarbons during two

reaction steps after a regeneration treatment. Results correspond to the CZ15 catalyst used at 350 ºC, regenerated through two different treatments: (i) sweeping with N_2 (2 h at 550 ºC) or; (ii) combustion of coke during a ramp temperature of 5 ºC min^{-1} from 350 to 550 ºC (**Figure 10a** and **10b**, respectively). The aging of coke under an inert or reductive atmosphere at high temperature is well-known,[62] but these possible modifications in coke structure do not allow for recovering any catalytic activity (**Figure 10a**). As observed, the conversion and yields at the beginning of the 2nd reaction cycle are practically overlapped with the last ones of the 1st cycle. Nevertheless, the catalyst totally recovers the activity of the fresh one after a regeneration treatment based on the combustion of coke under an air continuous flow during a ramp temperature between 350 and 500 ºC (**Figure 10b**). In the 2nd reaction cycle, the regenerated catalyst exhibits a perfectly reproducible evolution with time on stream of the conversion and product distribution.

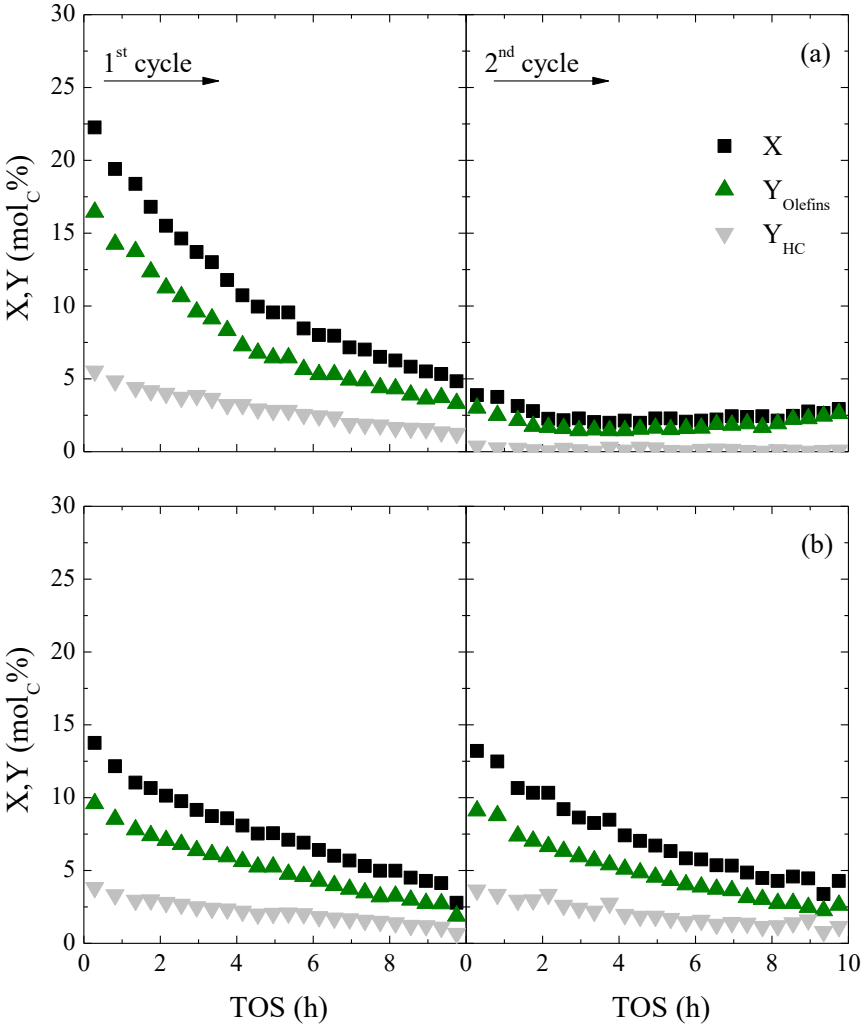

Figure 10. Evolution of the DME conversion and the yields of olefins and other hydrocarbon with time on stream in a reaction-regeneration cycle with CZ15 catalyst under the conditions: (a) 350 ºC; 1.0 g_{cat} h^{-1} mol_C $^{-1}$; regeneration through sweeping with N_2 at 550 ºC, 2 h; and (b) 350 ºC; 0.5 g_{cat} h^{-1} mol_C $^{-1}$; regeneration through coke combustion in air (temperature ramp from 350 to 550 ºC).

This regeneration treatment is likewise effective for recovering the activity of the CZ15 catalyst deactivated during a DTO run at 400 ºC (**Figure 11a,** with a regeneration ramp between 400 and 550 ºC), where the deactivation of the catalyst is much more severe (**Figure 3a**). At this higher temperature, the conversion decays faster, the total content

of coke is higher and it is mainly formed by coke fraction C3 (**Figure 4c**) deposited within the zeolite channels. Catalyst acidity does not significantly affect to the recovery of the activity, and CZ140 catalyst also presents similar conversion and yields in the 2nd reaction cycle at 400 ºC (**Figure 11b**). Therefore, independently of the content, location or nature of coke a combustion treatment with air based on a continuous heating from the reaction temperature (350 or 400 ºC) to 550 ºC totally recovers the initial activity of the catalyst.

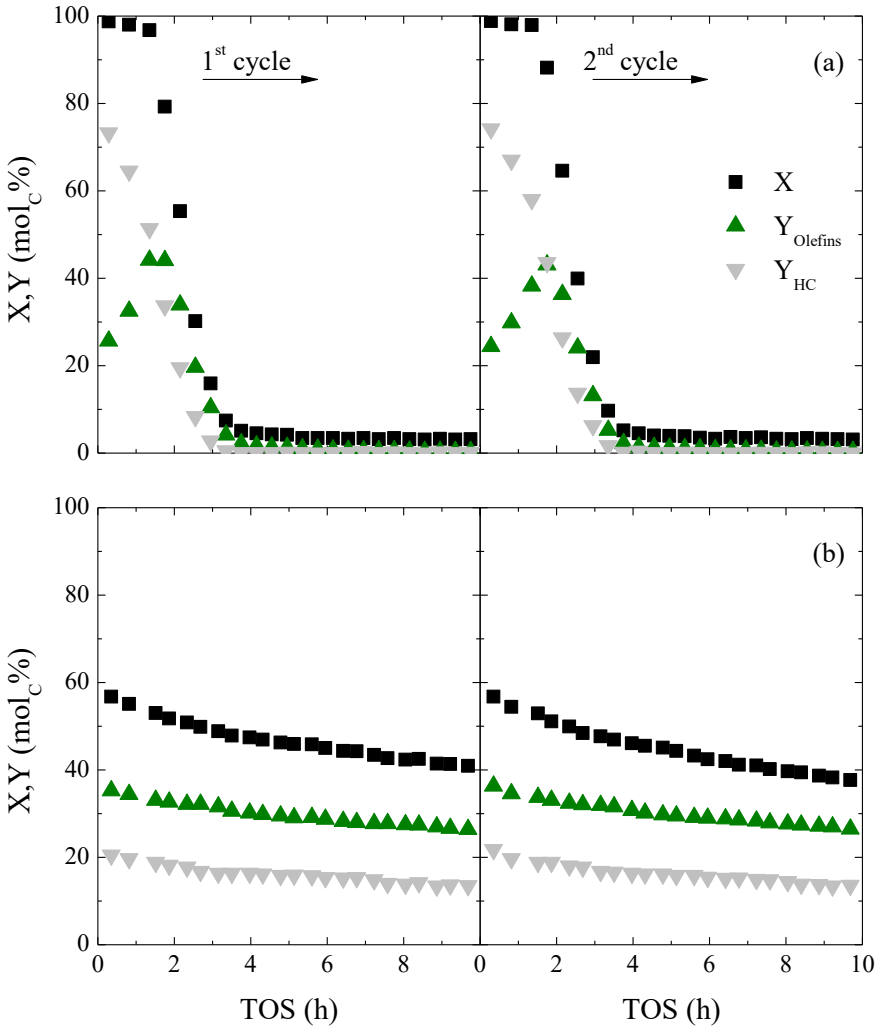

Figure 11. Evolution of the DME conversion and the yields of olefins and other hydrocarbon with time on stream in a reaction-regeneration cycle with (a) CZ15 catalyst

under the conditions: 400 ºC; 0.5 g_{cat} h^{-1} mol_C^{-1}; regeneration through coke combustion in air (temperature ramp from 400 to 550 ºC); and (b) Idem with CZ140 catalyst.

The results of this section highlight the relatively easy regeneration of the HZSM-5 zeolite-based catalyst deactivated during the DTO process, which is certainly interesting for its implementation. This is presumably attributed to the low condensation degree of the structures of coke, which is limited by the shape selectivity of the HZSM-5 zeolite. The attenuation of the bimolecular reaction of oligomerization, hydrogen transfer and condensation that yield coke is the main cause of the suitable performance of the zeolite.[55]

4. Conclusions

During dimethyl ether to olefins reaction, three different coke fractions are deposited on the HZSM-5 based catalyst prepared by the agglomeration of zeolite crystals with a mesoporous matrix of γ-Al_2O_3. The coke fractions are associated with carbonaceous structures located on the mesoporous matrix, the external surface and over the acidic sites within the micropores of the zeolite crystals. The presence of the matrix contributes to attenuate deactivation due to a favored evolution and deposition of coke on its mesoporous surface, thus reducing the blockage of the mouth of zeolite channels.

A clear influence of the catalyst acidity and the reaction conditions is observed on the amount and composition of the formed coke. An increase in the catalyst acidity and/or reaction temperature promotes the deposition of coke, which is explained by the higher activity of acidic sites for secondary reactions. Oligomerization, aromatization and

condensation pathways (associated with the alkene cycle mechanism) seem to have a notable effect on the formation of coke and thus, the catalyst deactivation.

An interesting strategy in order to attenuate the deposition of coke within the micropores of the zeolite is to co-feed water with DME. A steady state of olefin production is achieved using reaction temperature of 350 ºC because of the stable development of the arene cycle mechanism. However, this effect of water is restricted to scenarios in which the advance of the reaction is relatively low and it is not clearly effective using high acid catalyst and reaction temperatures of 400 ºC.

In any case, the low development of coke structures explains its total removal through combustion during a ramp temperature between 350 and 550 ºC. Catalyst completely recovers the activity, which is an important requirement for its use at industrial scale in similar reaction-regeneration units to that of MTO process.

Acknowledgments

This work was carried out with the support of the Ministry of Economy and Competitiveness of the Spanish Government, some cofounded with ERDF funds (CTQ2016-77812-R and CTQ2016-79646- P) and the Basque Government (IT748-13). T. Cordero-Lanzac also acknowledges the assistance of the Spanish Ministry of Education, Culture and Sport for the award of FPU grant (FPU15/01666).

References

(1) Sadrameli, S. M. Thermal/Catalytic Cracking of Liquid Hydrocarbons for the Production of Olefins: A State-of-the-Art Review I: Thermal Cracking Review. *Fuel* **2015**, *140*, 102–115.

(2) Sadrameli, S. M. Thermal/Catalytic Cracking of Liquid Hydrocarbons for the

Production of Olefins: A State-of-the-Art Review II: Catalytic Cracking Review. *Fuel* **2016**, *173*, 285–297.

(3) Seidel, C.; Jörke, A.; Vollbrecht, B.; Seidel-Morgenstern, A.; Kienle, A. Kinetic Modeling of Methanol Synthesis from Renewable Resources. *Chem. Eng. Sci.* **2018**, *175*, 130–138.

(4) De Falco, M.; Capocelli, M.; Centi, G. Dimethyl Ether Production from CO2rich Feedstocks in a One-Step Process: Thermodynamic Evaluation and Reactor Simulation. *Chem. Eng. J.* **2016**, *294*, 400–409.

(5) Ateka, A.; Pérez-Uriarte, P.; Gamero, M.; Ereña, J.; Aguayo, A. T.; Bilbao, J. A Comparative Thermodynamic Study on the CO2 Conversion in the Synthesis of Methanol and of DME. *Energy* **2017**, *120*, 796–804.

(6) Ateka, A.; Ereña, J.; Sánchez-Contador, M.; Perez-Uriarte, P.; Bilbao, J.; Aguayo, A. T. Capability of the Direct Dimethyl Ether Synthesis Process for the Conversion of Carbon Dioxide. *Appl. Sci.* **2018**, *8*, 677–690.

(7) Suwannapichat, Y.; Numpilai, T.; Chanlek, N.; Faungnawakij, K.; Chareonpanich, M.; Limtrakul, J.; Witoon, T. Direct Synthesis of Dimethyl Ether from CO2 Hydrogenation over Novel Hybrid Catalysts Containing a Cu–ZnO–ZrO2 Catalyst Admixed with WOx/Al2O3 Catalysts: Effects of Pore Size of Al2O3support and W Loading Content. *Energy Convers. Manag.* **2018**, *159*, 20–29.

(8) Olah, G. A.; Goeppert, A.; Prakash, G. K. S. Chemical Recycling of Carbon Dioxide to Methanol and Dimethyl Ether : From Greenhouse Gas to Renewable, Environmentally Carbon Neutral Fuels and Synthetic Hydrocarbons Chemical. *J. Org. Chem.* **2009**, *74*, 487–498.

(9) Catizzone, E.; Bonura, G.; Migliori, M.; Frusteri, F.; Giordano, G. CO2 Recycling to Dimethyl Ether: State-of-the-Art and Perspectives. *Molecules* **2018**, *23*, 31–58.

(10) Stangeland, K.; Li, H.; Yu, Z. Thermodynamic Analysis of Chemical and Phase Equilibria in CO2 Hydrogenation to Methanol, Dimethyl Ether, and Higher Alcohols. *Ind. Eng. Chem. Res.* **2018**, *57*, 4081–4094.

(11) Arcoumanis, C.; Bae, C.; Crookes, R.; Kinoshita, E. The Potential of Di-Methyl Ether (DME) as an Alternative Fuel for Compression-Ignition Engines: A Review. *Fuel* **2008**, *87*, 1014–1030.

(12) Marchionna, M.; Patrini, R.; Sanfilippo, D.; Migliavacca, G. Fundamental Investigations on Di-Methyl Ether (DME) as LPG Substitute or Make-up for Domestic Uses. *Fuel Process. Technol.* **2008**, *89*, 1255–1261.

(13) Faungnawakij, K.; Shimoda, N.; Viriya-empikul, N.; Kikuchi, R.; Eguchi, K. Limiting Mechanisms in Catalytic Steam Reforming of Dimethyl Ether. *Appl. Catal. B Environ.* **2010**, *97*, 21–27.

(14) Vicente, J.; Gayubo, A. G.; Ereña, J.; Aguayo, A. T.; Olazar, M.; Bilbao, J. Improving the DME Steam Reforming Catalyst by Alkaline Treatment of the HZSM-5 Zeolite. *Appl. Catal. B Environ.* **2013**, *130–131*, 73–83.

(15) Oar-Arteta, L.; Remiro, A.; Aguayo, A. T.; Bilbao, J.; Gayubo, A. G. Effect of Operating Conditions on Dimethyl Ether Steam Reforming over a CuFe2O4/γ-Al2O3 Bifunctional Catalyst. *Ind. Eng. Chem. Res.* **2015**, *54*, 9722–9732.

(16) Al-Dughaither, A. S.; De Lasa, H. Neat Dimethyl Ether Conversion to Olefins (DTO) over HZSM-5: Effect of SiO2/Al2O3on Porosity, Surface Chemistry, and Reactivity. *Fuel* **2014**, *138*, 52–64.

(17) Pérez-Uriarte, P.; Ateka, A.; Aguayo, A. T.; Bilbao, J. Comparison of HZSM-5 Zeolite and SAPO (-18 and -34) Based Catalysts for the Production of Light Olefins from DME. *Catal. Lett.* **2016**, *146*, 1892–1902.

(18) Pérez-Uriarte, P.; Ateka, A.; Gamero, M.; Aguayo, A. T.; Bilbao, J. Effect of the Operating Conditions in the Transformation of DME to Olefins over a HZSM-5 Zeolite Catalyst. *Ind. Eng. Chem. Res.* **2016**, *55*, 6569–6578.

(19) Bakare, I. A.; Muraza, O.; Sanhoob, M. A.; Miyake, K.; Hirota, Y.; Yamani, Z. H.; Nishiyama, N. Dimethyl Ether-to-Olefins over Aluminum Rich ZSM-5: The Role of Ca and La as Modifiers. *Fuel* **2018**, *211*, 18–26.

(20) Tian, P.; Wei, Y.; Ye, M.; Liu, Z. Methanol to Olefins (MTO): From Fundamentals to Commercialization. *ACS Catal.* **2015**, *5*, 1922–1938.

(21) Bjørgen, M.; Svelle, S.; Joensen, F.; Nerlov, J.; Kolboe, S.; Bonino, F.; Palumbo, L.; Bordiga, S.; Olsbye, U. Conversion of Methanol to Hydrocarbons over Zeolite H-ZSM-5: On the Origin of the Olefinic Species. *J. Catal.* **2007**, *249*, 195–207.

(22) McCann, D. M.; Lesthaeghe, D.; Kletnieks, P. W.; Guenther, D. R.; Hayman, M. J.; Van Speybroeck, V.; Waroquier, M.; Haw, J. F. A Complete Catalytic Cycle for Supramolecular Methanol-to-Olefins Conversion by Linking Theory with Experiment. *Angew. Chem. Int. Ed.* **2008**, *47*, 5179–5182.

(23) Ilias, S.; Bhan, A. Mechanism of the Catalytic Conversion of Methanol to Hydrocarbons. *ACS Catal.* **2013**, *3*, 18–31.

(24) Xu, S.; Zhi, Y.; Han, J.; Zhang, W.; Wu, X.; Sun, T.; Wei, Y.; Liu, Z. Advances in Catalysis for Methanol-to-Olefins Conversion. *Adv. Catal.* **2017**, *61*, 37–122.

(25) Haw, J. F.; Song, W.; Marcus, D. M.; Nicholas, J. B. The Mechanism of

Methanol to Hydrocarbon Catalysis. *Acc. Chem. Res.* **2003**, *36*, 317–326.

(26) Khadzhiev, S. N.; Magomedova, M. V.; Peresypkina, E. G. Mechanism of Olefin Synthesis from Methanol and Dimethyl Ether over Zeolite Catalysts: A Review. *Pet. Chem.* **2014**, *54*, 245–269.

(27) Wang, C.; Chu, Y.; Zheng, A.; Xu, J.; Wang, Q.; Gao, P.; Qi, G.; Gong, Y.; Deng, F. Newinsight into the Hydrocarbon-Pool Chemistry of the Methanol-to-Olefins Conversion over Zeolite H-ZSM-5 from GC-MS, Solid-State NMR Spectroscopy, and DFT Calculations. *Chem. Eur. J.* **2014**, *20*, 12432–12443.

(28) Olsbye, U.; Svelle, S.; Lillerud, K. P.; Wei, Z. H.; Chen, Y. Y.; Li, J. F.; Wang, J. G.; Fan, W. B. The Formation and Degradation of Active Species during Methanol Conversion over Protonated Zeotype Catalysts. *Chem. Soc. Rev.* **2015**, *44*, 7155–7176.

(29) Pérez-Uriarte, P.; Ateka, A.; Aguayo, A. T.; Gayubo, A. G.; Bilbao, J. Kinetic Model for the Reaction of DME to Olefins over a HZSM-5 Zeolite Catalyst. *Chem. Eng. J.* **2016**, *302*, 801–810.

(30) Pérez-Uriarte, P.; Ateka, A.; Gayubo, A. G.; Cordero-Lanzac, T.; Aguayo, A. T.; Bilbao, J. Deactivation Kinetics for the Conversion of Dimethyl Ether to Olefins over a HZSM-5 Zeolite Catalyst. *Chem. Eng. J.* **2017**, *311*, 367–377.

(31) Rojo-Gama, D.; Signorile, M.; Bonino, F.; Bordiga, S.; Olsbye, U.; Lillerud, K. P.; Beato, P.; Svelle, S. Structure–deactivation Relationships in Zeolites during the Methanol–to-Hydrocarbons Reaction: Complementary Assessments of the Coke Content. *J. Catal.* **2017**, *351*, 33–48.

(32) Forester, T. R.; Howe, R. F. In Situ FTIR Studies of Methanol and Dimethyl Ether in ZSM-5. *J. Am. Chem. Soc.* **1987**, *109*, 5076–5082.

(33) Yamazaki, H.; Shima, H.; Imai, H.; Yokoi, T.; Tatsumi, T.; Kondo, J. N. Direct Production of Propene from Methoxy Species and Dimethyl Ether over H-ZSM-5. *J. Phys. Chem. C* **2012**, *116*, 24091–24097.

(34) Li, Y.; Zhang, M.; Wang, D.; Wei, F.; Wang, Y. Differences in the Methanol-to-Olefins Reaction Catalyzed by SAPO-34 with Dimethyl Ether as Reactant. *J. Catal.* **2014**, *311*, 281–287.

(35) Gayubo, A. G.; Aguayo, A. T.; Olazar, M.; Vivanco, R.; Bilbao, J. Kinetics of the Irreversible Deactivation of the HZSM-5 Catalyst in the MTO Process. *Chem. Eng. Sci.* **2003**, *58*, 5239–5249.

(36) Aguayo, A. T.; Gayubo, A. G.; Atutxa, A.; Valle, B.; Bilbao, J. Regeneration of a HZSM-5 Zeolite Catalyst Deactivated in the Transformation of Aqueous Ethanol into Hydrocarbons. *Catal. Today* **2005**, *107–108*, 410–416.

(37) Wei, Y.; Yuan, C.; Li, J.; Xu, S.; Zhou, Y.; Chen, J.; Wang, Q.; Xu, L.; Qi, Y.; Zhang, Q.; et al. Coke Formation and Carbon Atom Economy of Methanol-to-Olefins Reaction. *ChemSusChem* **2012**, *5*, 906–912.

(38) Cordero-Lanzac, T.; Aguayo, A. T.; Gayubo, A. G.; Castaño, P.; Bilbao, J. Simultaneous Modeling of the Kinetics for N-Pentane Cracking and the Deactivation of a HZSM-5 Based Catalyst. *Chem. Eng. J.* **2018**, *331*, 818–830.

(39) Kanervo, J. M.; Krause, A. O. I.; Aittamaa, J. R.; Hagelberg, P. H.; Lipiäinen, K. J. T.; Eilos, I. H.; Hiltunen, J. S.; Niemi, V. M. Kinetics of the Regeneration of a Cracking Catalyst Derived from TPO Measurements. *Chem. Eng. Sci.* **2001**, *56*, 1221–1227.

(40) Keskitalo, T. J.; Lipiäinen, K. J. T.; Krause, A. O. I. Modelling of Carbon and Hydrogen Oxidation Kinetics of a Coked Ferrierite Catalyst. *Chem. Eng. J.* **2006**,

120, 63–71.

(41) Ochoa, A.; Ibarra, Á.; Bilbao, J.; Arandes, J. M.; Castaño, P. Assessment of Thermogravimetric Methods for Calculating Coke Combustion-Regeneration Kinetics of Deactivated Catalyst. *Chem. Eng. Sci.* **2017**, *171*, 459–470.

(42) Querini, C. A.; Fung, S. C. Temperature-Programmed Oxidation Technique: Kinetics of Coke-O2 Reaction on Supported Metal Catalysts. *Appl. Catal. A Gen.* **1994**, *117*, 53–74.

(43) Michels, N. L.; Mitchell, S.; Pérez-Ramírez, J. Effects of Binders on the Performance of Shaped Hierarchical MFI Zeolites in Methanol-to-Hydrocarbons. *ACS Catal.* **2014**, *4*, 2409–2417.

(44) Gayubo, A. G.; Alonso, A.; Valle, B.; Aguayo, A. T.; Bilbao, J. Selective Production of Olefins from Bioethanol on HZSM-5 Zeolite Catalysts Treated with NaOH. *Appl. Catal. B Environ.* **2010**, *97*, 299–306.

(45) Ibañez, M.; Pérez-Uriarte, P.; Sánchez-Contador, M.; Cordero-Lanzac, T.; Aguayo, A. T.; Bilbao, J.; Castaño, P. Nature and Location of Carbonaceous Species in a Composite HZSM-5 Zeolite Catalyst during the Conversion of Dimethyl Ether into Light Olefins. *Catalysts* **2017**, *7*, 254–266.

(46) Schulz, H. “Coking” of Zeolites during Methanol Conversion: Basic Reactions of the MTO-, MTP- and MTG Processes. *Catal. Today* **2010**, *154*, 183–194.

(47) Mores, D.; Kornatowski, J.; Olsbye, U.; Weckhuysen, B. M. Coke Formation during the Methanol-to-Olefin Conversion: In Situ Microspectroscopy on Individual H-ZSM-5 Crystals with Different Brønsted Acidity. *Chem. Eur. J.* **2011**, *17*, 2874–2884.

(48) Goetze, J.; Weckhuysen, B. M. Spatiotemporal Coke Formation over Zeolite

ZSM-5 during the Methanol-to-Olefins Process as Studied with: Operando UV-Vis Spectroscopy: A Comparison between H-ZSM-5 and Mg-ZSM-5. *Catal. Sci. Technol.* **2018**, *8*, 1632–1644.

(49) Bleken, F. L.; Barbera, K.; Bonino, F.; Olsbye, U.; Lillerud, K. P.; Bordiga, S.; Beato, P.; Janssens, T. V. W.; Svelle, S. Catalyst Deactivation by Coke Formation in Microporous and Desilicated Zeolite H-ZSM-5 during the Conversion of Methanol to Hydrocarbons. *J. Catal.* **2013**, *307*, 62–73.

(50) Müller, S.; Liu, Y.; Vishnuvarthan, M.; Sun, X.; Van Veen, A. C.; Haller, G. L.; Sanchez-Sanchez, M.; Lercher, J. A. Coke Formation and Deactivation Pathways on H-ZSM-5 in the Conversion of Methanol to Olefins. *J. Catal.* **2015**, *325*, 48–59.

(51) Leistner, K.; Nicolle, A.; Berthout, D.; da Costa, P. Kinetic Modelling of the Oxidation of a Wide Range of Carbon Materials. *Combust. Flame* **2012**, *159*, 64–76.

(52) Pérez-Uriarte, P.; Gamero, M.; Ateka, A.; Díaz, M.; Aguayo, A. T.; Bilbao, J. Effect of the Acidity of HZSM-5 Zeolite and the Binder in the DME Transformation to Olefins. *Ind. Eng. Chem. Res.* **2016**, *55*, 1513–1521.

(53) Al-Dughaither, A. S.; de Lasa, H. HZSM-5 Zeolites with Different SiO2 /Al2O3 Ratios. Characterization and NH3 Desorption Kinetics. *Ind. Eng. Chem. Res.* **2014**, *53*, 15303–15316.

(54) Khare, R.; Liu, Z.; Han, Y.; Bhan, A. A Mechanistic Basis for the Effect of Aluminum Content on Ethene Selectivity in Methanol-to-Hydrocarbons Conversion on HZSM-5. *J. Catal.* **2017**, *348*, 300–305.

(55) Guisnet, M.; Magnoux, P. Organic Chemistry of Coke Formation. *Appl. Catal. A*

Gen. **2001**, *212*, 83–96.

(56) Guisnet, M.; Costa, L.; Ribeiro, F. R. Prevention of Zeolite Deactivation by Coking. *J. Mol. Catal. A Chem.* **2009**, *305*, 69–83.

(57) Dai, W.; Wu, G.; Li, L.; Guan, N.; Hunger, M. Mechanisms of the Deactivation of SAPO-34 Materials with Different Crystal Sizes Applied as MTO Catalysts. *ACS Catal.* **2013**, *3* (4), 588–596.

(58) Dai, W.; Cao, G.; Yang, L.; Wu, G.; Dyballa, M.; Hunger, M.; Guan, N.; Li, L. Insights into the Catalytic Cycle and Activity of Methanol-to-Olefin Conversion over Low-Silica AlPO-34 Zeolites with Controllable Brønsted Acid Density. *Catal. Sci. Technol.* **2017**, *7* (3), 607–618.

(59) Aguayo, A. T.; Gayubo, A. G.; Atutxa, A.; Olazar, M.; Bilbao, J. Catalyst Deactivation by Coke in the Transformation of Aqueous Ethanol into Hydrocarbons. Kinetic Modeling and Acidity Deterioration of the Catalyst. *Ind. Eng. Chem. Res.* **2002**, *41*, 4216–4224.

(60) Gayubo, A. G.; Aguayo, A. T.; Morán, A. L.; Olazar, M.; Bilbao, J. Role of Water in the Kinetic Modeling of Catalyst Deactivation in the MTG Process. *AIChE J.* **2002**, *48*, 1561–1571.

(61) Mier, D.; Gayubo, A. G.; Aguayo, A. T.; Olazar, M.; Bilbao, J. Olefin Production by Cofeeding Methanol and N-Butane: Kinetic Modeling Considering the Deactivation of HZSM-5 Zeolite. *AIChE J.* **2011**, *57*, 2841–2853.

(62) Aguayo, A. T.; Gayubo, A. G.; Ereña, J.; Atutxa, A.; Bilbao, J. Coke Aging and Its Incidence on Catalyst Regeneration. *Ind. Eng. Chem. Res.* **2003**, *42*, 3914–3921.

Abstract Graphics